doi:10.1246/cl.2011.1340

Published on the web November 12, 2011

Quaternary-ammonium-bearing Aromatic Surfactants: Effect of the Alkyl Chain Positions on Their Micelle and DNA-complex Structures

Takuma Matsuo, Shota Fujii, Yumi Kamikawa, Tomoki Nishimura, Yusuke Sanada, Shinichi Mochizuki, and Kazuo Sakurai*
Department of Chemistry and Biochemistry, The University of Kitakyushu, 1-1 Hibikino, Wakamatsu-ku, Kitakyushu, Fukuoka 808-0135

(Received August 17, 2011; CL-110683; E-mail: sakurai@kitakyu-u.ac.jp)

The isomeric effect was investigated for a newly synthesized series of quaternary aromatic ammoniums with alkyl chains of different substitution position. Their micellar and DNA-complex structures were investigated with synchrotron small-angle X-ray scattering and isomeric effect is discussed. For the dodecyloxy tail, the meta–meta showed a hexagonally packed cylinder, while the meta–para formed a lamella. After addition of DNA, both showed a lamella with DNA sandwiched between the surfactant bilayers.

Lipids or synthetic surfactants exhibit a wide range of self-assembled structures in aqueous solutions, determined by their chemical structures as well as concentrations and ionic strength.[1] Chemical variations in the hydrophobic tails and the hydrophilic headgroups lead to enormous richness and complexity in structures.[2] Recently, the ionic complexes made from cationic surfactants (CSs) and DNA have been extensively studied to apply gene delivery.[3,4] These complexes also show structural richness and, most importantly, their DNA-delivering efficiency is reported as being closely related to the complex structures.[3,5–8] Thus, correlating the chemical variations to both micelles and DNA complex structures are of importance in terms of fundamental and application standpoints. In this article, we prepared a series of aromatic cationic surfactants bearing a quaternary ammonium as the headgroup and two alkyl chains as the tails. By changing their substitution positions (i.e., meta and meta versus meta and para) as well as the tail length from 9, 12, and 18 carbons, we examined how the isomerism[9,10] affects the micelle itself and DNA/CS complex structures.

[3,5-Bis(dodecyloxy)benzyl]trimethylammonium (denoted by QAmm12, the suffix number denotes the number of carbon atoms in the tail, Figure 1A) and its isomer [3,4-bis(dodecyloxy)benzyl]trimethylammonium (denoted by QAmp12) were synthesized as described in the Supporting Information (Figure S1[16]). Their analogs with different tail lengths ($n = 9$ and 18) were also prepared. The compounds were first dissolved in chloroform and vacuum-dried in a vial. After addition of aqueous NaCl solution (50 mM), the micellar formation was promoted by sonicating for 10 min. The resultant solution was almost transparent in the concentration range of <5 mM. The detecting of micelles in solution was performed by fluorescence measurements. We used 8-anilino-1-naphthalenesulfonic acid (ANS) as a fluorescence probe. The fluorescence measurements of all samples were carried out with a fluorescence spectrophotometer by exciting at 385 nm and recording the emission spectrum in the range 400–700 nm. Figure 1B plots the alkyl chain-length dependence of the critical micellar concentration (CMC) for both compounds. With increase of the chain length,

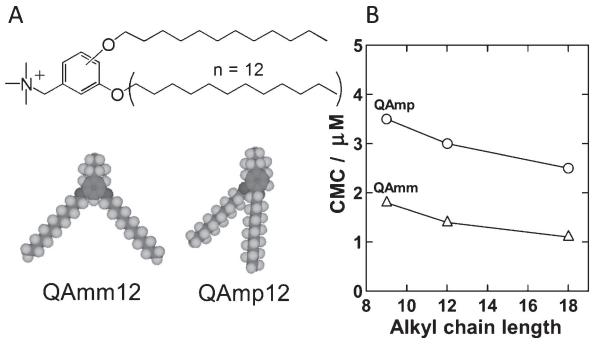

Figure 1. Chemical structures and their CPK models for QAmm12 and its isomer QAmp12 and the alkyl chain length dependence of CMC in 50 mM NaCl.

CMC decreased as expected. QAmp showed about twofold larger CMC than QAmm for all samples. This difference can be related to the fact that QAmm has a higher symmetry than QAmp as depicted in CPK model in the figure. An increase in symmetry of the surfactants leads to increased levels of π-stacking of aromatic rings. This in turn leads to a lowering of the CMC and conversely lower levels of symmetry lead to a higher CMC. De et al.[11] reported that the position of aromatic segments in the single-tailed surfactant is significantly related to CMC. The present data demonstrates that the tail-substituted position is also important to determine CMC.

Figure 2 presents small-angle X-ray scattering (SAXS) profiles for QAmm and QAmp with $n = 9$ and 12, measured at SPring-8 Beamline 40B2. For $n = 18$, both QAmm and QAmp showed polymorphism and no reproducibility in SAXS and thus they are not discussed.

QAmp9 exhibited a typical feature for a mono-bilayer, which was confirmed by AFM (Figure S4[16]), and thus the profile was fitted by a plate model with reasonable parameters: the head and alkyl thicknesses of 0.38 and 2.30 nm (Figure S2[16]). The profile from QAmm9 seems to consist of a bilayer scattering and crystalline diffraction peaks. The presence of the diffraction indicates that QAmm9 can take a more ordered structure in atomic scale than its isomer of QAmp9, which could be related to the lower CMC and higher symmetry of this compound. The fitting the bilayer scattering gave the head and alkyl thicknesses of 0.38 and 1.60 nm (Figure S2[16]).

QAmp12 showed several sharp diffraction peaks and a large up-turn in the small q. The peak positions satisfied the relation of 1:2:3:4, indicating the formation of lamellar. This is confirmed by TEM (Figure S4[16]). From the peak positions; the lamellar spacing was determined to be 3.9 nm, which was much larger than the bilayer thickness of QAmp9. Figure 2A presents the

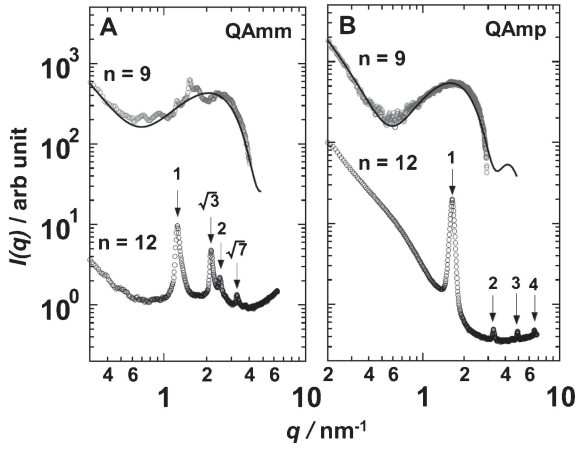

Figure 2. SAXS profiles from QAmm (A) and QAmp (B) with $n = 9$ and 12. The solid lines are best fitted plate models and the numbers attached to the peaks show peak position ratios for hexagonally packed cylinder and lamella. The lipid concentration was 5.0 mM (0.3 wt %) in 50 mM NaCl.

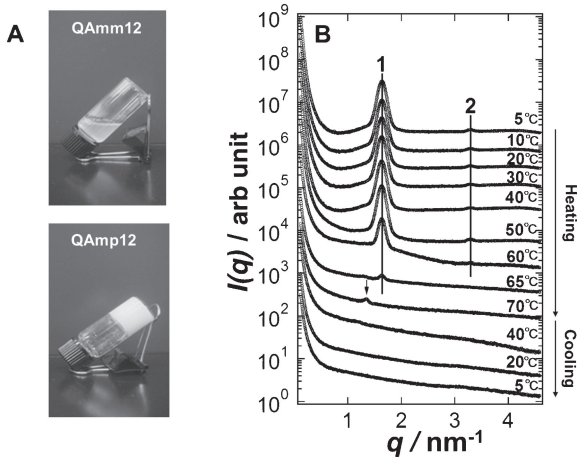

Figure 3. A photo of the aqueous gel made from QAmp12 compared with its isomer QAmm12 (A) and temperature dependence of SAXS profiles from QAmp12 at 5 mM. First, the SAXS measurements were performed upon heating from 5 to 70 °C over 80 min and then cooling from 70 to 5 °C over further 60 min.

scattering from QAmm12, showing the diffraction peaks due to hexagonally packed cylinders. The intercylinder distance was determined to be 5.9 nm.

It should be noted that the isomerism between QAmm12 and QAmp12 leads to completely different micellar aggregate structures, even before adding DNA, as presented in Figure 2. Such isomeric effect on micellar structures has been reported in several papers.[9,10] The CPK models in Figure 1 show that the tails of QAmm12 are spread out wider than QAmp12. On the analogy of the packing parameter theory,[2] QAmm12 is considered to take an inverted cylinder as illustrated in Figure 5A.

When the concentration was increased to 10 mM or more for QAmp12 and the solutions were left for a few days, they became gelatinized as presented in Figure 3, while QAmm12 showed turbidity but did not become gelatinized. When the temperature was increased above 70 °C, the solution became transparent and

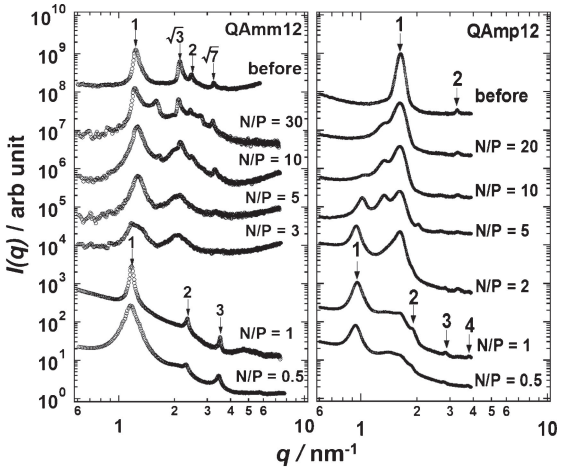

Figure 4. SAXS changes upon addition on DNA.

Table 1. Characteristic dimensions determined with SAXS

Sample code	Distance or thickness/nm	Lamellar spacing/nm at N/P = 1.0
QAmm9	2.4[a]	4.8
QAmm12	5.9[b]	5.4
QAmp9	3.1[a]	—
QAmp12	3.9[c]	6.6

[a]Bilayer thickness determined with the model fitting. [b]Intercylinder distance from the diffraction peak positions. [c]Lamellar distance from the diffraction peak positions.

the gel disappeared. When we measured the SAXS profiles upon heating and subsequent cooling (Figure 3B), the lamellar peaks disappeared between 60 and 65 °C, being consistent with the appearance changes. When we cooled down to 5 °C, there was no peak observed for 30 min, but the same peak then appeared after a few days. This observation shows that the formation of the lamella is a very slow process. When we measured wide-angle X-ray scattering from a QAmp12 solution, comparing with the powder of QAmp12, the diffraction peaks appeared in the same positions (Figure S3[16]), showing that the local structure formed in the gel is the same in its solid crystal, being similar to other gelators.[12,13] This type of gel is called "dray gel" and essentially consists of entangled long needle crystals.[14]

Figure 4 compares how the addition of DNA (sonicated salmon sperm extracted with phenol, bp ≈3000) alters the SAXS scattering profiles. For QAmm12, the hexagonal peaks changed to lamellar ones at N/P = 1 and there was no intermediate structure nor polymorphism observed. On the other hand, when DNA was added to QAmp12 at N/P = 5–20, there were several peaks observed at $q = 1.7$ and 2.0 nm^{-1} and these cannot be assigned. These additional peaks disappeared at N/P = 2, where the noninteracting lamellar and new peaks coexist and the new peaks became dominate at N/P = 1 and 0.5 and the structure of DNA/QAmp12 can be assigned to another lamella with a larger spacing than before addition of DNA. The increment of the spacing is 2.7 nm, which is reasonable assuming that DNA (diameter of 2 nm) was intercalated between two bilayers made of QAmp12.

Table 1 summarizes the characteristic dimensions determined with SAXS, and Figure 5 illustrates structural changes

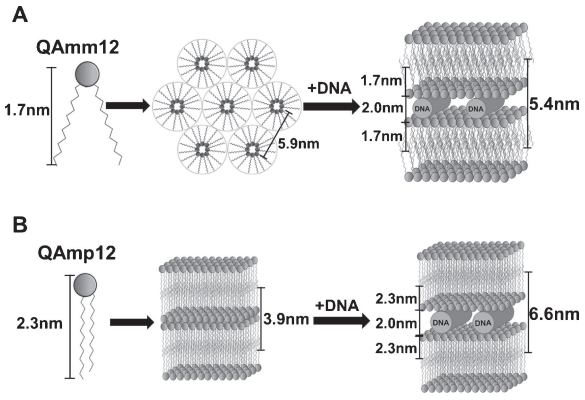

Figure 5. Schematic illustration for the self-assembled and DNA-complexed structures for QA with $n = 12$.

upon addition of DNA for $n = 12$. From $n = 9$ to 12 for QAmp, the bilayer thickness was increased by 0.8 nm and this increment almost equates to twice the fully extended length of C_3H_6. After complexation, the lamellar spacing was increased by 0.6 nm from $n = 9$ to 12, being consistent with previous studies for an aromatic surfactant with a different head group.[15]

When compared with QAmp12 and QAmm12 after complexation with DNA, the latter showed a longer lamellar spacing by 1.2 nm than the former. As presented in the figure, for both cases, the lamellar spacing almost equals the summation of the DNA diameter and the sizes of the two molecules calculated with MOPAC, assuming that the tails are fully stretched. The agreement is good enough to conclude that the molecular assembling models presented in the figure are reasonable.

In conclusion, the isomerism in QAmm and QAmp induces a dramatic difference in both micellar assembling and DNA-complexed structures. The former showed a hexagonally packed cylinder, while the latter a lamella. After complexation with DNA, both show a sandwiched lamella, but the spacing is different.

All SAXS experiments were carried out at SPring-8 Beamline 40B2 (No. 2010A1432) and the present work is financially supported by JST CREST.

References and Notes

1 G. Tresset, *PMC Biophys.* **2009**, *2*, 3.
2 J. N. Israelachvili, *Intermolecular and Surface Forces*, Academic Press, London, **1992**, Vol. 450.
3 a) K. Ewert, N. L. Slack, A. Ahmad, H. M. Evans, A. J. Lin, C. E. Samuel, C. R. Safinya, *Curr. Med. Chem.* **2004**, *11*, 133. b) K. Ewert, A. Ahmad, H. M. Evans, C. R. Safinya, *Expert Opin. Biol. Ther.* **2005**, *5*, 33.
4 *Nonviral Vectors for Gene Therapy*, ed. by L. Huang, M.-C. Hung, E. Wagner, Academic Press, London, UK, **1999**.
5 R. Koynova, L. Wang, R. C. MacDonald, *Proc. Natl. Acad. Sci. U.S.A.* **2006**, *103*, 14373.
6 R. Koynova, L. Wang, Y. Tarahovsky, R. C. MacDonald, *Bioconjugate Chem.* **2005**, *16*, 1335.
7 a) M. Sakuragi, K. Koiwai, K. Nakamura, H. Masunaga, H. Ogawa, K. Sakurai, *J. Phys.: Conf. Ser.* **2011**, *272*, 012011. b) M. Sakuragi, S. Kusuki, E. Hamada, H. Masunaga, H. Ogawa, I. Akiba, K. Sakurai, *J. Phys.: Conf. Ser.* **2009**, *184*, 012008.
8 K. Koiwai, K. Tokuhisa, R. Karinaga, Y. Kudo, S. Kusuki, Y. Takeda, K. Sakurai, *Bioconjugate Chem.* **2005**, *16*, 1349.
9 I. Tucker, J. Penfold, R. K. Thomas, C. C. Dong, S. Golding, C. Gibson, I. Grillo, *Langmuir* **2011**, *27*, 6674.
10 S. Bogusz, R. M. Venable, R. W. Pastor, *J. Phys. Chem. B* **2000**, *104*, 5462.
11 S. De, V. K. Aswal, S. Ramakrishnan, *Langmuir* **2010**, *26*, 17882.
12 O. Gronwald, K. Sakurai, R. Luboradzki, T. Kimura, S. Shinkai, *Carbohydr. Res.* **2001**, *331*, 307.
13 *Molecular Gels: Materials with Self-Assembled Fibrillar Networks*, ed. by R. G. Weiss, P. Terech, Springer, Tokyo, **2006**.
14 a) Y. Jeong, A. Friggeri, I. Akiba, H. Masunaga, K. Sakurai, S. Sakurai, S. Okamoto, K. Inoue, S. Shinkai, *J. Colloid Interface Sci.* **2005**, *283*, 113. b) Y. Jeong, K. Hanabusa, H. Masunaga, I. Akiba, K. Miyoshi, S. Sakurai, K. Sakurai, *Langmuir* **2005**, *21*, 586.
15 T. Nishimura, T. Cho, A. M. Kelley, M. E. Powell, J. S. Fossey, S. D. Bull, T. D. James, H. Masunaga, I. Akiba, K. Sakurai, *Bull. Chem. Soc. Jpn.* **2010**, *83*, 1010.
16 Supporting Information is available electronically on the CSJ-Journal Web site, http://www.csj.jp/journals/chem-lett/index.html.

